First VLTI-MIDI direct determinations of asteroid sizes*

M. Delbo
UNS, CNRS, Observatoire de la Côte d'Azur, BP 4229 06304 Nice cedex 04 - France.
INAF-Osservatorio Astronomico di Torino Strada Osservatorio 20, 10025 Pino Torinese, Torino - Italy
delbo@oca.eu

S. Ligori
INAF-Osservatorio Astronomico di Torino Strada Osservatorio 20, 10025 Pino Torinese, Torino - Italy

A. Matter
UNS, Observatoire de la Côte d'Azur, BP 4229 06304 Nice cedex 04 - France.

A. Cellino
INAF-Osservatorio Astronomico di Torino Strada Osservatorio 20, 10025 Pino Torinese, Torino - Italy
and

J. Berthier
Institut de Mecanique Celeste (IMCCE) 77 av. Denfert Rochereau - 75014 Paris - France

ABSTRACT

We have obtained the first successful interferometric measurements of asteroid sizes and shapes by means of VLTI-MIDI. VLTI can spatially resolve asteroids in a range of sizes and heliocentric distances that are not accessible to other techniques such as adaptive optics and radar. We have observed, as a typical bench mark, the asteroid (951) Gaspra, visited in the past by the Galileo space probe, and we derive a size in good agreement with the ground truth coming from the *in situ* measurements by the Galileo mission. Moreover, we have also observed the asteroid (234) Barbara, known to exhibit unusual polarimetric properties, and we found evidence of a potential binary nature. In particular, our data are best fit by a system of two bodies of 37 and 21 km in diameter, separated by a center-to-center distance of ∼24 km (projected along the direction of the baseline at the epoch of our observations).

Subject headings: minor planets, asteroids; techniques: interferometric; infrared: solar system

1. Introduction

The study of the physics of asteroids is crucial to constrain models of formation, growth and physical properties of the planetesimals that accreted into the inner Solar System planets.

Most asteroids are too small to allow a direct determination of their fundamental physical properties including sizes [1], shapes, and masses

*Based on data obtained at the Very Large Telescope Interferometer (VLTI) of the European Southern Observatory (ESO): program ID 076.C-0798.

[1] Only for the largest hundred main belt asteroids their sizes can be directly measured with present day adaptive optics systems at 10–m class telescopes (Conrad et al. 2007)

[2]. According to current expectations, in the next decade, the Gaia mission of the European Space Agency will provide accurate mass determinations for about 100 of the largest main belt asteroids (MBAs) and will be able to directly measure the sizes of all MBAs larger than 30 km ($\sim 1,000$ objects) (Mouret et al. 2007; Mignard et al. 2007). At present, however, the most important source of progress in this field is related to the increasing rate of discovery of binary systems. These discoveries have been made possible by adaptive optics imaging at several large telescopes, radar – particularly suited for the study of near-Earth objects (NEAs) – and optical lightcurve observations. Binary asteroids are extremely important to derive the mass of the system; sizes and shapes of the components are then needed to estimate average densities, which in turn provide crucial information about the internal structure of the bodies.

Unfortunately, asteroid sizes are generally not measurable by means of direct imaging. Improvements in the performances of modern adaptive optics systems are currently making significant progress, but this is forcedly limited to size measurements of the largest MBAa, and very close approaching NEAs (Conrad et al. 2007). Radar has been proven to be a powerful tool to infer shapes and sizes for a sample of km– and sub–km–sized objects. This technique, however, is mostly limited to the population of NEAs, which can experience close encounters with our planet. This is due to the fact that the intensity of the radar echo decreases with the fourth power of the distance.

To summarize, the vast majority of asteroid sizes, due to their small apparent angular extension and orbital location in the Main Belt, remain beyond the range of measurability using current techniques. As a consequence, nearly all of the available information we have today about asteroid sizes comes from the results of indirect methods of size determination.

The most widely adopted technique to determine asteroid sizes is thermal infrared radiometry (see Harris and Lagerros 2002, and references therein). This method is based on the fact that the infrared flux $I(\lambda)$ carries information about the size of the source. In particular, $I(\lambda)$ is proportional to the area of the asteroid visible to the observer. However, $I(\lambda)$ depends also upon the temperature distribution on the asteroid surface. Different models of asteroid thermal infrared emission (the so–called asteroid thermal models; see §2, Harris and Lagerros 2002; Delbo and Harris 2002, and references therein) are used to estimate the surface temperature distribution allowing one to derive D from measurements of $I(\lambda)$. The asteroid's geometric visible albedo, p_V, can then be obtained from Eq. (1) which represents the fundamental relation linking the effective diameter, D (in km), the albedo, and the absolute magnitude H (the magnitude in the V–band that would be measured by observing the object at 1 AU distance from both the Sun and the observer, and at zero phase angle):

$$\log p_V = 6.247 - 2\log D - 0.4H \qquad (1)$$

We note that the value of p_V is *per se* a very important physical parameter, because it is a function of the composition, texture and roughness of an asteroid's surface. Polarimetric observations can also be used to estimate the value of p_V (Muinonen et al. 2002; Cellino et al. 2005) from empirical relations between the albedo and the degree of polarization of the reflected light from the asteroid surface. The asteroid effective diameter D can then be determined from p_V using Eq. (1).

We note that the value of the absolute magnitude H is derived from photometric observations of the asteroid under different illumination conditions (Muinonen et al. 2002). However, in practice, the H–value is usually not determined at the same time of radiometric or polarimetric observations. Its value is in most circumstances simply taken from public catalogs, such as the Minor Planet Center's orbital database, which are known to be affected by significant systematic errors of 0.3 magnitudes or more, mainly for asteroids smaller than ∼40–50 km (Cellino et al. 2008; Parker et al. 2008).

As a conclusion, it can be said that there are currently significant uncertainties on the size (and albedo) values for MBAs of moderate sizes (D <50km): all but about a thousand of the over one million asteroids in the main belt are smaller than 50 km.

[2]At the time of writing, only fifteen multiple main belt asteroids had their components resolved, allowing determination of their orbits and thus of the masses of the systems (Marchis et al. 2008)

There is thus a strong need to extend direct size measurements to smaller asteroids. However, this is a very challenging task. The only technique that has been so far nominally available, namely the measurement of stellar occultations, is hardly applicable in practice due to the very narrow strips of observability of occultation events and to the actual limits in current accuracies of stellar astrometric catalogues and of asteroid orbital elements (see Tanga and Delbo 2007).

As we show in this paper, a new very powerful facility for the direct measurement of asteroid sizes is now available, namely the Very Large Telescope Interferometer (VLTI) of the European Southern Observatory (ESO). In particular, VLTI can be successfully applied to objects that (i) are not too big (apparent angular diameters $\lesssim$ 100–200 mas), but, on the other hand, (ii) are sufficiently bright (brighter than visible magnitude $\sim$13 –14). Although these constraints certainly limit the number of objects for which VLTI can provide direct size and shape determinations, a large number of asteroids still exist that fall within the above magnitude and size ranges (see Fig. 1 and Delbo et al. 2006; Loreggia et al. 2008). The results presented in this paper, based on our pilot program, are a nice confirmation of the above statement.

Generally speaking, VLTI has the capability of measuring sizes (and shapes) of asteroids from measurements of the visibility (contrast) of interferometric fringes. Visibility is a function of the apparent angular extension of the body along the projected interferometer baseline. At present, visibilities can be measured at the VLTI in the near infrared (1-2.5 μm) using the Astronomical Multi-BEam combineR (AMBER; Petrov and The AMBER Consortium 2003) and in medium infrared (N-band) by means of the Mid-Infrared Interferometric Instrument (MIDI; Leinert et al. 2003; Przygodda et al. 2003). Because VLTI baseline lengths vary between 16 and 120 m, spatial resolutions of λ/B between about 2 and 12 mas and 20 and 200 mas can be in principle obtained with AMBER and MIDI, respectively. For a general technical overview of the VLTI, see for instance Glindemann et al. (2003). Details of the VLTI instruments can also be found on the ESO web pages: http://www.eso.org/projects/vlti/.

One particularly interesting feature of the MIDI instrument, is that it also measures the total (non coherent) spectral energy distribution, $I(\lambda)$, of the source in the 8-13 μm spectral interval. This thermal infrared data can then be used to derive asteroid sizes, through the application of asteroid thermal models (see e.g. Harris and Lagerros 2002; Delbo and Harris 2002, and references therein).

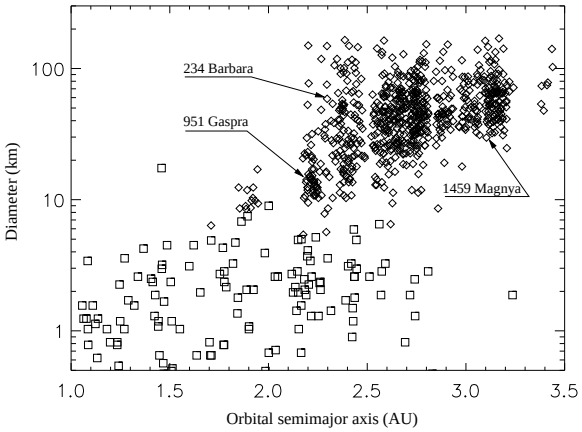

Fig. 1.— Asteroids for which MIDI can provide direct size determination, according to the present instrument requirements: i.e *i*) a correlated thermal infrared flux (flux $\times$ visibility) at 11.8 μm greater or equal to 1 Jy and *ii*) a visibility greater or equal to 0.1. Diamonds: MBAs. Squares: NEAs. Orbital element are from the Minor Planet Center (MPC). Diameters have been calculated from the MPC H values assuming an average albedo of 0.2. Ephemerides have been calculated every 5 days for NEAs and every 15 days for MBAs for a time span of 15 years starting from June 1, 2005, to check for those bodies meeting conditions *i* and *ii*.

In this paper we report the results of the first successful observations of asteroids with VLTI-MIDI. In particular, the selected targets were (951) Gaspra and (234) Barbara.

For (951) Gaspra we have *a priori* detailed information of the size and shape: this object was flown–by by the space mission Galileo on its way to Jupiter (Thomas et al. 1994). This target was selected with the purpose of performing a test of the real performances of the MIDI–VLTI system, by comparing the results of our size determination, with the ground truth coming from the *in situ* measurements by the Galileo space probe.

As for (234) Barbara, this asteroid belongs to a rare taxonomic class (*Ld*) and has been discovered by one of us to exhibit a very anoma-

lous behavior in terms of polarimetric properties (Cellino et al. 2006) (in more technical terms, this object displays a phase-polarization curve that reaches strongly negative values at unusually large phase angles, larger than 20°). These properties have been until recently unique, whereas a handful of other relatively small objects belonging to the same or other unusual taxonomic classes have been recently found to share the same polarimetric behavior (Gil-Hutton et al. 2008). Interestingly, (234) Barbara has a long rotation period (26.5 hours, Schober 1981; Harris and Young 1983) which might be suggestive of a possible binary system. The effective diameter derived from IRAS radiometric is of 44±1 km (Tedesco et al. 2002) which implies a geometric albedo (p_V) of 0.22±0.01 when an absolute magnitude H=9.02 is assumed. Taken at face value, the polarimetric parameters of this object would give an albedo (p_V) of ∼0.325 (Cellino et al. 2006), quite larger than the IRAS value. However, Cellino et al. (2006) claim that the unique polarimetric behavior of this object should prevent anyone from using usual polarization - albedo relations to infer reliable albedo estimates for this asteroid.

This paper is organized as follows: In §2 we describe the theoretical models used for the interpretation of MIDI data; we present details of MIDI observations of (951) Gaspra and (234) Barbara in §3 along with the adopted data reduction procedure; results are presented in §4, followed by a discussion (§5) and a concluding (§6) section.

2. Analysis of MIDI observations

The main purpose of MIDI is to combine coherently the infrared light collected by two of the four 8m UT telescopes (or by two of the four AT telescopes) of the ESO VLT: both telescopes observe the same target and when the optical path distances of the two beams are equal, interferometric fringes form on the detector. Fringe contrast (the ratio between the maximum and the minimum intensity) carries information on the angular extension of the source. More precisely, MIDI measures the source's spatial coherence function or interferometric visibility. Given the brightness distribution $O(x, y, \lambda)$ of a source on the projected sky plane, (x,y), and the corresponding total flux intensity $I(\lambda) = \iint O(x, y, \lambda)dxdy$, the visibility is given by: $V(u, v) = \hat{O}(u, v)/I(\lambda)$, where $\hat{O}(u, v) = \iint O(x, y, \lambda)e^{-2\pi i(xu+yv)}dxdy$ is the Fourier transform of $O(x, y, \lambda)$; $u = B_x/\lambda$ and $v = B_y/\lambda$ are the spatial frequencies in rad^{-1} along the x and y coordinates respectively; B_x and B_y are the components along the two orthogonal directions of the interferometer's baseline projected on the plane of the sky; λ is the wavelength of the light.

For maximum sensitivity, MIDI observations are usually carried in dispersed mode: a prism, with a spectral resolution R ≃30, and a long slit inserted along the optical path allows visibility measurements to be obtained simultaneously at different wavelengths in the spectral range between 8 and 13 μm. Because $V \equiv V(u = B_x/\lambda, v = B_y/\lambda)$, obtaining V at different λ is also equivalent to a variation of the baseline length at constant λ.

In principle, by measuring $V(u, v)$ for a set of different values of u and v, possibly filling the uv-plane, one could directly derive the spatial flux distribution of the source $O(x, y, \lambda)$, by taking the inverse Fourier transform of $V(u, v)$ (aperture synthesis). However, because at present the MIDI acquisition of one calibrated visibility observation requires about one hour of time when observations are executed in service mode, images of asteroids from interferometric measurements are difficult to obtain from aperture synthesis methods. An additional complication comes also from the fact that asteroids rotate considerably during such an interval of time.

When visibility measurements are available at only one or few baselines, which is the most common observing circumstance, simple parametric model-fitting techniques must be used. In the following we describe two geometric models used to derive the sizes of our targets from MIDI visibility measurements, namely a disk of uniform intensity and a binary system made of two uniform disks.

We also used simple models of asteroid thermal emission (see Harris and Lagerros 2002) in order to derive the sizes of our targets from the MIDI spectrophotometry only (Figs. 1b and 2b). Theoretical visibilities calculated from these models with asteroid sizes fixed to the values derived from spectrophotometry were afterwards compared to the measured visibilities.

Uniform disk model

If the image of the asteroid on the plane of the sky is approximated by a uniform circular disk of angular diameter θ, the amplitude of the visibility as a function of $u = B/\lambda$ is given by:

$$|V_\theta(u)| = |2J_1(\pi\theta u)/(\pi\theta u)|\,, \qquad (2)$$

where J_1 is the first-order Bessel function of first kind and B is the length of the baseline projected on the plane of the sky. The angular diameter of the disk can be derived from a single visibility measurement. The equivalent uniform disk diameter $\tilde{D}$ of the asteroid is then trivially derived from θ, and the known geocentric distance Δ of the body. Note that for a highly irregularly-shaped body (such as (951) Gaspra), θ and $\tilde{D}$ correspond to the angular and the physical extension of the body along the projected baseline (see Fig. 4).

Binary system model

Since the rate of discovery of binary systems has been steadily increasing in recent years, and the detection/characterization of binary systems is a primary application of high-resolution techniques such as the VLTI, it is worth developing a model of a binary source to be applied to the analysis of VLTI data. Here, we assume that the image on the plane of the sky, projected along the baseline B of a binary asteroid system is given by two uniform disks of diameters θ_1 and θ_2 separated by an angular distance ρ (with the corresponding physical diameters $\tilde{D}_1$, $\tilde{D}_2$, and physical separation a): $O_b(x,\lambda) = O_{\theta_1}(x,\lambda) + \delta(x-\rho) \otimes O_{\theta_2}(x,\lambda)$, where $\otimes$ is the convolution operator and the x coordinate is taken along the baseline, in this case.

As mentioned above, the visibility function is the Fourier Transform of $O_b(x,\lambda)$ divided by the total flux intensity I: namely $V_b = [\hat{O}_{\theta_1} + \hat{O}_{\theta_2} \exp(-i2\pi u\rho)]/I$. Because $\hat{O}_\theta = V_\theta I_\theta$, $I = I_{\theta_1} + I_{\theta_2}$, and $\theta_1^2/\theta_2^2 = I_{\theta_1}/I_{\theta_2}$, we can derive an analytical expression for the visibility amplitude of the binary asteroid by inserting these equations in the modulus of V_b: after a little algebra, we get:

$$|V_b(u)| = \frac{\sqrt{V_{\theta_1}^2 I_{\theta_1}^2 + V_{\theta_2}^2 I_{\theta_2}^2 + 2V_{\theta_1} I_{\theta_1} V_{\theta_2} I_{\theta_2} \cos(2\pi u\rho)}}{I} \qquad (3)$$

Note that Eq. 3 is a function of the three parameters θ_1, θ_2, and ρ. These parameters are adjusted (e.g. by means of Monte Carlo procedure) until the χ^2 between the model ($V_b(u)$) and the observed ($V(u_i)$) visibilities is minimized, where $\chi^2 = \sum_{i=0}^{N} \left((V_b(u_i) - V(u_i))^2 / \sigma^2_{V(u_i)} \right)$.

Asteroid thermal models

In order to interpret thermal infrared observations of asteroids, models of the temperature distribution and corresponding infrared emission at the surface of these objects have been developed. Sophisticated thermo-physical asteroid models are nowadays used when information about the body's shape and spin vector are known. Infrared fluxes are then computed as function of the asteroid's albedo, thermal inertia and macroscopic roughness, and these parameters are then adjusted until a best-fit to the data is obtained (see Mueller 2007; Delbo and Tanga 2008, for details).

In the most common situation of bodies for which spin vector and shape information is not available, simplified thermal models based on an assumed spherical shape must be adopted. In the case of our MIDI data, the refined Standard Thermal Model (STM, Lebofsky et al. 1986), the Near–Earth Asteroid Thermal Model (NEATM, Harris 1998), and the Fast Rotating thermal Model (FRM, see Harris and Lagerros 2002; Delbo and Harris 2002, and references therein) were used to fit the measured photometric infrared fluxes in order to derive the diameters and the albedos of (951) Gaspra and (234) Barbara.

In a second step, interferometric visibilities were also computed by taking the Fourier transform along the projected baseline spatial infrared emission of the STM, FRM, and NEATM using the sizes derived from MIDI spectro–photometry only. Models visibilities were then compared to the measured ones (see Figs. 1a and 2a).

Without entering into details at this stage, we remind the reader that the STM has been found to be most appropriate for the large MBAs. In the case of small fast-rotators, like some near-Earth objects, the surface temperature distribution is not well reproduced by the STM. The FRM, or even better the NEATM, are better suited. The NEATM is mostly an improved version of STM, in which the value of the so-called "beaming pa-

rameter", one of the parameters of the model, is not arbitrarily fixed like in the case of STM, but it is actually derived from the data taken in different thermal IR bands. This leads usually to a much better fit of the measured thermal IR data. The corresponding relative errors are generally less than 15% in diameter and 30% in albedo. For a more detailed description of the uncertainties on diameters and albedos when derived from the NEATM, STM and FRM see (Delbo et al. 2003; Delbo 2004; Harris 2006).

3. MIDI observations and data reduction

The observations of (234) Barbara and (951) Gaspra were carried out in service mode, on November 15, 2005 between 07 and 08 UT, and on November 14, 2005 between 05 and 06 UT, respectively. A typical observing sequence with MIDI is described extensively by Przygodda et al. (2003). Three consecutive visibility measurements were obtained for (951) Gaspra, whereas in the case of (234) Barbara only one visibility observation was acquired. Table 1 reports the observational circumstances for the two targets including their phase angle, and their heliocentric and geocentric distances, for each visibility measurement [3]. Interferometric fringes were detected in all cases, demonstrating the feasibility of ground-based interferometric observations of Solar System minor bodies for the first time.

In the case of (234) Barbara and (951) Gaspra the 47m-long interferometric baseline was used by coherently combining the light from the UT2 (KUEYEN) and UT3 (MELIPAL) telescopes (UT2–UT3 baseline). Table 2 gives the value of the projected baseline and other relevant parameters during the observations of our targets. The telescopes and the delay lines of the interferometer were tracked at the rates predicted from the ephemerides of each target. Our observations included medium-infrared photometric standard stars and visibility calibrators chosen from the ESO database, namely HD 31421 for (951) Gaspra and HD 2324 for (234) Barbara. Absolutely calibrated infrared spectra for the calibration stars were taken from the database of Cohen et al. (1999). Absolutely calibrated fluxes for the target asteroids were obtained by multiplying the ratio target/calibration star raw counts at each wavelength by the absolute fluxes of the calibration stars. Instrumental target visibilities were obtained by the ratio of the source raw correlated flux and the source raw photometric flux. Calibrated visibilities were calculated by dividing the instrumental visibility of the target asteroid and the one of the corresponding calibrator star. Calibrators are stars have small and known angular diameter, so that their visibility is close to unity at all wavelengths. Figures 2 and 3 show the resulting calibrated interferometric visibilities, as well as the measured thermal IR fluxes of (951) Gaspra and (234) Barbara, respectively. The predicted interferometric visibilities corresponding to different size solutions resulting from the different models of §2 are also shown in the figures. Different thermal models give correspondingly different predictions of the interferometric visibilities.

Visibility measurements can be extracted from MIDI observations by using two different data reduction software packages, namely the MIDI Interactive Analysis (MIA) or the Expert WorkStation (EWS). MIA does a power spectrum analysis (or incoherent analysis) of the MIDI dispersed fringes in order to obtain one visibility "spectrum" for each exposure. On the contrary, EWS performs a coherent analysis of the dispersed fringes and enables one to obtain, in addition to the visibility, the phase of fringes as a function of λ.
The data of both asteroids were reduced by using in parallel MIA and EWS. The use of both packages gives indications of the visibility uncertainties. At the beginning of the data reduction, the 2-dimensional frames in the raw data files are converted to 1-dimensional spectra. As a first step, both MIA and EWS use masks to select those regions of the detector where fringes (coherent flux) and photometric images (photometric incoherent fluxes) of the source form. By default, EWS uses a pre-defined mask which always selects the region of the detector where the signals of the fringes and photometric channels are expected to be present. The MIA mask is defined by searching the spectrum on the detector and performing a Gaussian

[3]Note that we observed during an exceptionally close opposition of (951) Gaspra, and that these are not very frequent.Last such favorable opposition, with (951) Gaspra at a geocentric distance, $\Delta < 1$ AU took place on September 2008. Next ones will take place in December 2015, October 2018, November 2028, September 2031, December 2038, October 2041, and November 2051.

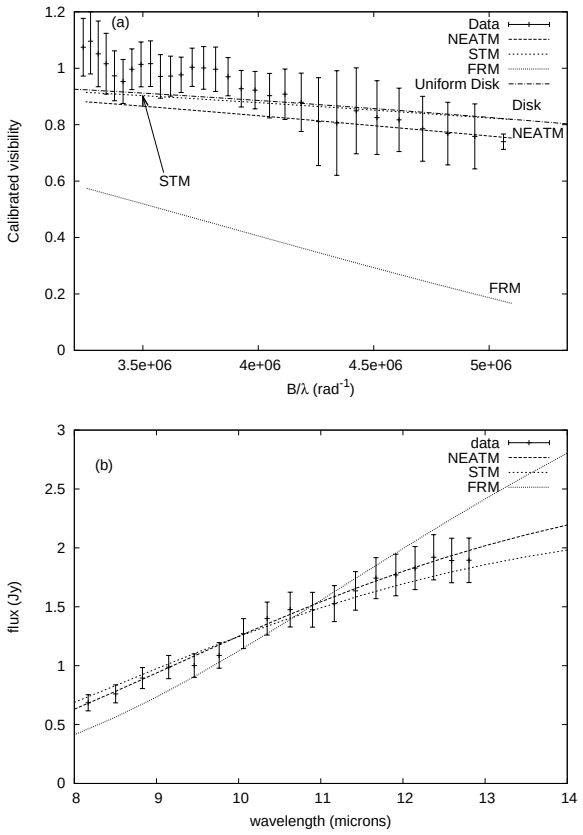

Fig. 2.— (a): the observed interferometric visibility data for (951) Gaspra, and the corresponding best–fit by means of a uniform disk model. The NEATM, STM, and FRM curves are the predicted interferometric visibility derived from the three thermal model solutions obtained from the measured infrared fluxes in the range between 8 and 13 μm (measured visibilities were not used in the thermal models fits). (b): the measured thermal infrared fluxes at different wavelengths, and the corresponding best–fit solutions by means of the three thermal models described in the text.

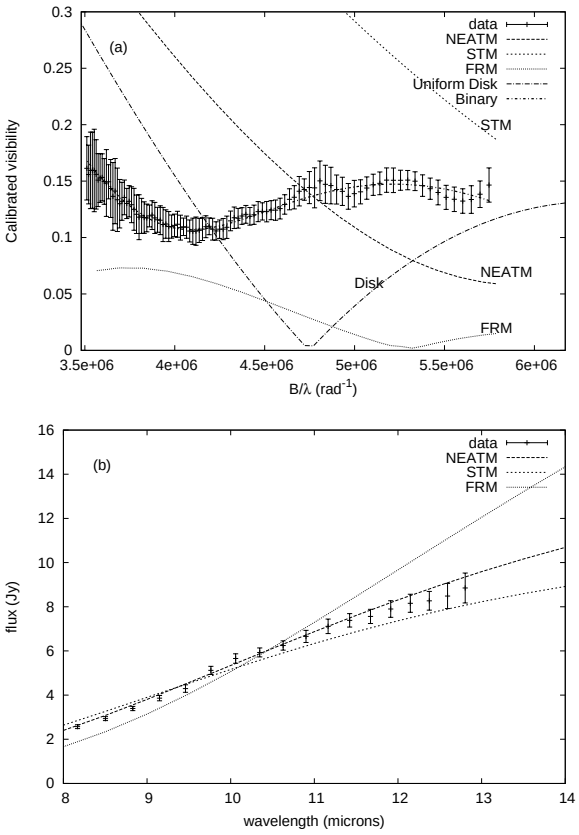

Fig. 3.— The same as Figure 2, but for (234) Barbara. In (a), in addition to the interferometric visibility predicted by a uniform disk model and to the thermal model solutions, the best–fit interferometric visibility of the binary model (see text) is also plotted. Note how the latter model produces a clearly much better fit to the observations than the others.

fit over the signal in order to parameterize its position and width. When faint sources are observed, the MIA mask might have trouble finding the position of the signals on the detector. This was the case for (951) Gaspra and consequently the pre-defined EWS mask was used. Because (234) Barbara was brighter, the MIA mask was used without problems to extract the fringes and the photometric images.

Suppression of the sky background, which is the predominant flux contribution in N–band, is an issue. Sky background generates a DC offset of the whole spectrum. This DC component creates a fringe artifact at zero OPD (Optical Path Difference between the two beams) when EWS calculates the Fourier transform of the measured signal dispersed along wavelengths on the detector, in order to estimate the fringe position. If the source is weak and so is the signal within the fringe, the artifact at zero OPD may be considered as the real fringe by EWS. As our sources are weak and the fringe tracking was not performed around the zero OPD, we used an option of EWS (dAve) to remove the DC background component of the signal by subtracting the mean of all pixels in the spectrum from each individual pixel.

Moreover, at the end of the data reduction process of MIA, the calculated visibilities turned out to be quite noisy. Since we do not request high spectral resolution we modified the λ binning (the default value is 3 pixels for each spectral channel) to 8 pixels for the calculation of the visibilities.

In the next section we describe how asteroid physical parameters were derived from MIDI measurements.

4. Results

Asteroid sizes were derived from the application of the models described in section §2 to MIDI measurements. First of all, the STM, the FRM, and the NEATM were fit to the measured infrared fluxes $I(\lambda)$ only, to obtain effective diameters. Flux data and thermal models' best–fit continua for (951) Gaspra and (234) Barbara are plotted in Fig. 2 and Fig. 3 respectively. The geometric visible albedos were calculated from the derived sizes, utilizing H values from the Minor Planet Center, namely H=11.46 for (951) Gaspra and H=9.02 for (234) Barbara. Table 4 reports D and p_V obtained from the application of the thermal models and the corresponding angular extension of the body at the time of our VLTI observation. An uncertainty of 0.5 magnitudes (see Cellino et al. 2008), affecting the uncertainty on the derived albedo, was assumed on the adopted value of the absolute magnitude H (from the MPC).

We then computed interferometric visibilities corresponding to the obtained NEATM, STM and FRM solutions (by using the values of the diameters and the albedos obtained from models fits to the infrared fluxes). We calculated the Fourier transform of the model thermal infrared emission and evaluated this function at ($u = B\cos\theta_B, v = B\sin\theta_B$). The values of B and θ_B are reported in Tab. 2 for each VLTI observation. The predicted interferometric visibilities corresponding to the different thermal radiometry solutions are over–plotted along with the measured values in Fig. 2 and 3 as the three dotted lines labeled NEATM, STM, and FRM.

In a second step, we used the simple geometric models described in §2 to analyze measured visibilities:

(951) Gaspra

Fringes were detected for all interferometric observations reported in Tab. 1 and Tab. 2. However, by careful analysis of the acquisition images, we discovered a failure in the acquisition of the source during the first MIDI measurement (the one taken at UT 03:21:43). So, we limited our analysis to the second and the third observations, only. In order to increase the signal to noise ratio of the visibility measurements, we computed the average visibility extracted using the EWS mask between the second and third measurement (i.e. those obtained at 04:29:28 and 05:04:27 UT). Figure 2 shows the obtained data points. The error bars correspond to half of the difference between the two measurements.

We note that for $B/\lambda \lesssim 3.8 \times 10^6 \mathrm{rad}^{-1}$, corresponding to $\lambda \gtrsim 11\mu m$, Fig. 2 shows that the visibility oscillates around 1, which we interpret as due to lack of spatial resolution at these wavelengths.

We performed a least square fit of Eq. (2) (uniform disk model) to the data points of Fig. 2 using θ as the only free parameter and using B = 41.64m. We obtain θ=17±2 mas, which corresponds to $\tilde{D}$=11±1 km at the distance of the asteroid. (see Tab. 3 for a summary of our results). The comparison of our VLTI/MIDI size determination of (951) Gaspra with the asteroid's projected size known from Galileo spacecraft observations are discussed in §5.

(234) Barbara

The visibility of (234) Barbara extracted from MIDI observations are shown in Fig. 3. Error bars, obtained using the EWS data reduction software, represent the standard deviation of the visibility. As for the case of (951) Gaspra, a least square fit of Eq. (2) was performed to the data points with the angular diameter θ of the uniform disk as the only free parameter. We obtained θ=51.0±0.4 mas, which corresponds to $\tilde{D}$=44.6±0.3 km at the distance of the asteroid. However, Fig. 3 clearly shows that a uniform disk model provides a poor fit to the measurements. Model visibilities calculated by means of the NEATM, the STM, and the FRM thermal models also give a poor fit of the actual measurements. This is likely an indication that the spa-

tial distribution of the source's infrared flux differs from that of uniform single body.

An application of the binary disk model to the measured visibility, however, gives much better results. In this case, we found a remarkably good match between the model and the observations, as shown in Fig. 3. Best fit values of the model parameters θ_1, θ_2, and ρ are 43.0±0.5, 24.2±0.2, and 28.1±0.2 mas, respectively. When we take into account the distance to the asteroid at the time of our observations we derive diameters of $\tilde{D}_1$=37.1±0.5 km and $\tilde{D}_2$=21.0±0.2 km for the primary and the secondary components of the binary system. The distance center to center projected on the interferometer baseline was of a=24.2±0.2 km.

5. Discussion

For (951) Gaspra we have *a priori* information of its size, shape and spin vector state from spacecraft observations (Thomas et al. 1994). This is the main reason why we decided to observe this object, in order to obtain a reliable estimate of the resulting accuracy in the size determination from thermal models and by means the uniform disk model fit to MIDI interferometric observations. We caution here that a single uniform disk model may provide a poor description of the spatial distribution of the infrared emission of asteroids in some cases, as clearly demonstrated by our observations of (234) Barbara.

In order to estimate the reliability of our size determinations of (951) Gaspra, we compared the sizes derived from our MIDI measurements with that published by Thomas et al. (1994). As a first step, we computed the orientation of the shape of the asteroid at the epoch of the VLTI observation using an asteroid physical ephemerides service of the Institut de Mécanique Celeste et de Calcul des Ephemerides (IMCCE) in Paris [4]. The shape model of the asteroid, derived from the Galileo spacecraft observations, is that of Thomas et al. (1994). Two spin vector models are available, namely a first one with $\alpha_p = 9.5°$, $\delta_p = 26.7°$ (Thomas et al. 1994) and a second one with $\lambda_p = 20°$, $\beta_p = 19°$ (Kaasalainen et al. 2001), where α_p and δ_p are J2000 equatorial coordinate of the asteroid's pole, whereas λ_p and β_p are its J2000 ecliptic longitude and latitude. Figure 4 shows the orientation of (951) Gaspra, assuming the spin model 1, at the time of the second and the third visibility measurement. Note that the asteroid was observed almost pole–on. Figure 5 shows a comparison of the object shape model adopted and one image taken by the Galileo mission.

From the shape model, we found that total projected area visible to the observer was 380 mas^2. Taking $2 \times \sqrt{380.0/\pi}$ we obtain a value of θ_D=22 mas corresponding to D=14.71 km. Thomas et al. (1994) give detailed information about the accuracy of the shape model: from their Fig. 5 one can estimate a conservative error of 1 km along the projected radius of the shape model of (951) Gaspra at the time of our observation. We can take 15±2 km as the value for D from Thomas et al. (1994) shape model. When we compare this latter value with the size solutions derived from thermal models, we find a very good agreement with estimate of D from the NEATM. Even though the NEATM was developed for the observation of relatively small near-Earth asteroids, there is no reason to believe that it should not be suited to apply also to main belt asteroids of the same size, and this is confirmed by our MIDI data of (951) Gaspra.

As for the other thermal models, the STM predicts a fairly smaller diameter, whereas the size estimate of the FRM turns out to be very inaccurate. The latter result is not surprising: given the pole–on aspect of the asteroid with respect to the sun, the effect of rotation and thermal inertia in smoothing out the surface temperature is strongly reduced, and the ideal circumstances for the application of the FRM are certainly not met.

Figure 4 shows also the orientation of the projected baseline of the interferometer. The angular extension of (951) Gaspra was 19.5, and 16.9 mas, respectively. From Thomas et al. (1994), Fig. 5 one can estimate an error of 2 km in the shape model along the direction of the VLTI projected baseline. This value correspond to 3 mas at the distance of the asteroid. We can thus take 19±3 mas and 17±3 mas as the extensions of the shape of (951) Gaspra at the time of the second and the third visibility measurement, respectively.

Assuming the pole solution of Kaasalainen et

[4] Internet service available at http://www.imcce.fr → Ephemerides → Ephemeris for physical observation of the solar bodies.

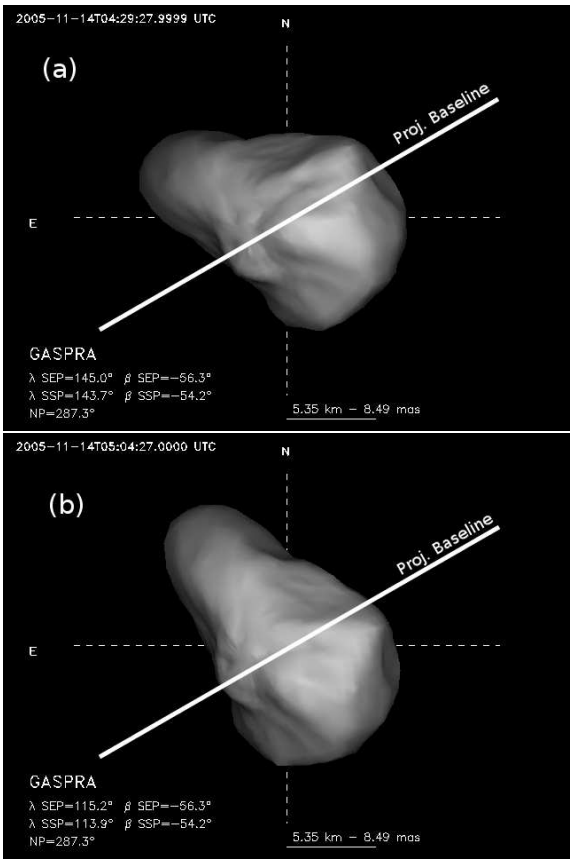

Fig. 4.— Shape model of (951) Gaspra projected on the plane of the sky at the time of the second (a) and third (b) VLTI visibility measurement, computed using the MOVIS software.

al. (2001) (model 2) the difference in total projected area of the asteroid visible to the observer with respect to the pole solution 1 turns out to be negligible. The size of (951) Gaspra along the projected baseline, however, turns out to be 17±3 mas at the time of both the second and the third visibility measurement using the Kaasalainen et al. (2001) pole.

The result of this analysis indicates that the expected value of the projected size of (951) Gaspra along the VLTI baseline at the epochs of our observations is in excellent agreement with the angular extension of the body derived from fitting the uniform disk model to the MIDI measurements, i.e. 17±2 mas.

Our MIDI observations of (234) Barbara strongly suggest that this asteroid is composed by two bodies with diameters of 37 and 21 km. We note that, taken at face value, the separation of ∼24 km between the centers of the two disks is smaller than the sum of the radii of the two bodies of ∼ 29 km. This might be an indication of a bi-lobated shape. On the other hand, because the separation of the two objects is measured along the projected baseline on the plane of the sky, the actual distance between the two components can be much larger, implying a binary system, as shown on Fig. 6. At the moment, we are not able to distinguish between the possibility that (234) Barbara is a single object having a bi-lobated shape, or it is actually a detached or contact binary system. Further interferometric observations using different projected baselines coupled with optical lightcurve measurements are required to test the different possible alternatives.

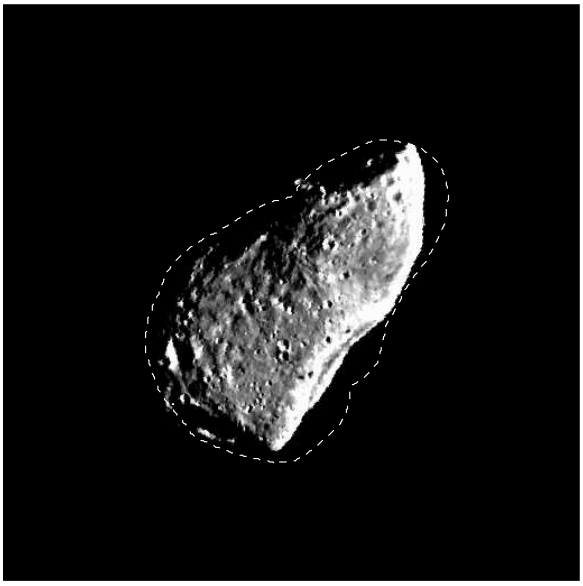

Fig. 5.— Comparison of an image of (951) Gaspra taken by the Galileo mission on 1991-10-29 at 22:26 UT from a distance of 5300 km and our shape model (dashed line) observed under the same circumstances. The scale of the image is 54m/pixel.

In order to compare the size of (234) Barbara derived from the geometric binary model and those obtained from thermal modeling, we compare the diameters of the spheres with equivalent area, D. The total surface of the binary model varies from 1420±30 km^2 corresponding to the fully separated case, to 1370±30 km^2 when the

center-to-center distance of the two disks is 29 km. These values correspond to D of 43±1 km and 42±1 km, respectively and they lie in between the NEATM and the STM size estimates.

6. Conclusions

We have obtained the first direct measurements of asteroid sizes from ground based interferometry in the thermal infrared using MIDI of the ESO VLTI. Our observations of (951) Gaspra convincingly show that MIDI observations can spatially resolve asteroids as small as ∼12 km in the Main Belt with an excellent accuracy. This is suggested by the comparison of our VLTI results with the shape model obtained by means of *in situ* imaging observations during the fly–by of the Galileo mission. Our observations suggest that second target, (234) Barbara, is a potential binary system. However, further investigation are required to fully prove this hypothesis and to derive the geometric parameters of the system (in particular, the separation of the two components, which might also be in contact).

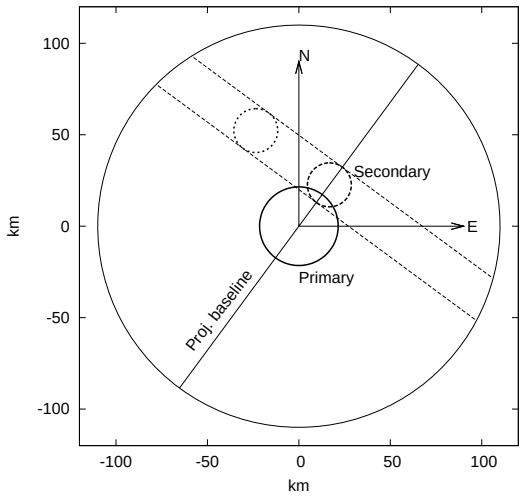

Fig. 6.— Sketch of the binary model for the asteroid (234) Barbara resulting from VLTI–MIDI observations. The most external circle represents the width of the 10μm–beam of the UT telescopes in which the source must be positioned in order to provide an interferometric signal measurable by MIDI. The secondary component of the system can be anywhere within the two dashed lines perpendicular to the interferometer projected baseline.

We note that a binary nature of (234) Barbara is not surprising given the slow rotation period of this object obtained in the past from lightcurve observations. A binary nature, however, can not explain *per se* the unusual polarimetric properties of this object (Cellino et al. 2006). The above properties are most likely due to an unusual surface composition of this object, as also suggested by its unusual taxonomic classification. We have here a very interesting example of an object which seems to exhibit clear evidence of a complex history, and this makes it a high-priority target for further observations and theoretical investigations.

Acknowledgments

We thank the staff and the Science Archive Operation of the European Southern Observatory (ESO), and in particular Markus Wittkowski. The comments and suggestions from an anonymous referee are gratefully acknowledged. The work of Marco Delbo (MDB) has been supported by the European Space Agency (ESA). This research was partially carried out while MDB was a Henri Poincaré Fellow at the Observatoire de la Côte dAzur. The Henri Poincaré Fellowship is funded by the CNRS-INSU, the Conseil Général des Alpes-Maritimes and the Rotary International – District 1730

MDB wishes to thank O. Chesneau, M. Zio for valuable comments and discussions and D. Licchelli for having made at disposal the set of lightcurves of (951) Gaspra obtained quasi simultaneously to the MIDI observations.

REFERENCES

Bowell, E., Hapke, B., Domingue, D., Lumme, K., Peltoniemi, J., and Harris, A. W. 1989. In Asteroids II (R. P. Binzel et al., eds.), Univ. of Arizona, Tucson, 524.

Cellino, A., Belskaya, I. N., Bendjoya, P., di Martino, M., Gil-Hutton, R., Muinonen, K., Tedesco, E. F. 2006. Icar, 180, 565.

Cohen, M., Walker, R. G., Carter, B., Hammersley, P., Kidger, M., Noguchi, K. 1999. AJ, 117, 1864.

Conrad, A. R., et al. 2007. Icar, 191, 616.

Delbo, M. and Tanga, P. 2008. P&SS, in press.

Delbo, M., Dell'Oro, A., Harris, A. W., Mottola, S., Mueller, M. 2007. Icar, 190, 236.

Delbo, M., et al. 2006. Icar, 181, 618.

Delbo M. 2004. Freie Universitaet Berlin, Digitale Dissertation. on-line at: http://www.diss.fu-berlin.de/2004/289/indexe.html

Delbo, M., Harris, A. W., Binzel, R. P., Pravec, P., Davies, J. K. 2003. Icar, 166, 116.

Delbó, M., & Harris, A. W. 2002, M&PS, 37, 1929

Cellino, A., Dell'Oro, A., Tedesco, E. F. 2008. P&SS, in press.

Cellino, A., Gil-Hutton, R., Di Martino, M., Bendjoya, Ph., Belskaya, I. N., & Tedesco, E. F. 2005. Icar, 179, 304.

Gil-Hutton, R., Mesa, V., Cellino, A., Bendjoya, P., Peñaloza, L., Lovos, F. 2008. A&A 482, 309.

Glindemann, A., et al. 2003. Ap&SS, 286, 35.

Harris, A. W. 2006. Asteroids, Comets, Meteors 229, 449.

Harris, A. W., Lagerros, J. S. V. 2002. In: Bottke, W.F., Cellino, A., Paolicchi, R.P., Binzel, P. (Eds.), Asteroids III. Univ. of Arizona Press, Tucson, 205.

Harris, A. W. 1998. Icar, 131, 291.

Harris, A. W., Young, J. W. 1983. Icar 54, 59.

Kaasalainen, M., Torppa, J. and K. Muinonen 2001. Icar, 153, 37.

Lebofsky, L. A., et al. 1986. Icar, 68, 239.

Leinert, C., et al. 2003. Ap&SS, 286, 73.

Loreggia, D., Delbo, M., Gai, M., Lattanzi, M. G., Ligori, S., Saba, L., Wittkowski, M., & Cellino, A. 2008, The Power of Optical/IR Interferometry: Recent Scientific Results and 2nd Generation, 565.

Marchis, F., Descamps, P., Baek, M., Harris, A. W., Kaasalainen, M., Berthier, J., Hestroffer, D., Vachier, F. 2008. Icar, 196, 97.

Mignard, F., et al. 2007. EM&P, 101, 97.

Mouret, S., Hestroffer, D., Mignard, F. 2007. Asteroid masses and improvement with Gaia. A&A, 472, 1017.

Muinonen, K., Piironen, J., Shkuratov, Y. G., Ovcharenko, A., Clark, B. E. 2002. In: Bottke, W.F., Cellino, A., Paolicchi, R.P., Binzel, P. (Eds.), Asteroids III. Univ. of Arizona Press, Tucson, 123.

Mueller, M. 2007. Freie Universitaet Berlin, Digitale Dissertation, on-line at: http://www.diss.fu-berlin.de/2007/471/indexe.html

Parker, A., Ivezić, Ž., Jurić, M., Lupton, R., Sekora, M. D., Kowalski, A. 2008. The size distributions of asteroid families in the SDSS Moving Object Catalog 4. Icarus 198, 138-155.

Petrov, R. G., et al. 2003. Ap&SS, 286, 57.

Przygodda, F., Chesneau, O., Graser, U., Leinert, C., Morel, S. 2003. Ap&SS, 286, 85.

Schober, H. J. 1981. A&A, 96, 302.

Tanga, P., Delbo, M. 2007. A&A, 474, 1015.

Thomas, P. C., Veverka, J., Simonelli, D., Helfenstein, P., Carcich, B., Belton, M. J. S., Davies, M. E., Chapman, C. 1994. Icar, 107, 23.

Tedesco, E. F., Noah, P. V., Noah, M., Price, S. D. 2002. AJ, 123, 1056.

This 2-column preprint was prepared with the AAS LaTeX macros v5.2.

Asteroid	Date	UT	r (AU)	Δ (AU)	α (deg)
Barbara	2005-11-15	07:21:05	2.1297371	1.2051145	12.6
Gaspra	2005-11-14	03:21:43	1.8566048	0.8685061	02.2
Gaspra	2005-11-14	04:29:28	1.8566492	0.8685798	02.3
Gaspra	2005-11-14	05:04:27	1.8566857	0.8686429	02.3

Table 1: Observational circumstances and relevant data. Asteroid ephemerides were generated using the JPL Horizons System: http://ssd.jpl.nasa.gov/?horizons. r and Δ are the heliocentric and geocentric distances of the targets; α is the solar phase angle (the Sun-Target-Observer angle).

Asteroid	Telescopes	B (m)	θ_B (deg)	RA	DE
(234) Barbara	UT2-UT3	46.285	36.41	03:57:51.40	-08:03:33.2
(951) Gaspra (1)	UT2-UT3	34.730	59.85	03:03:22.65	+20:47:46.0
(951) Gaspra (2)	UT2-UT3	40.495	58.75	03:03:19.79	+20:47:24.2
(951) Gaspra (3)	UT2-UT3	42.785	56.35	03:03:17.45	+20:47:06.1

Table 2: VLTI configuration and other relevant interferometric parameters of the performed observations. B is the length in m of the baseline projected on the plane of sky; θ_B is its position angle from North to East. RA and DEC are the J2000 Right Ascension and the Declination of the targets at the time of the observations.

Asteroid	D (km)	θ (mas)	Notes
Gaspra	11±1	17±2	EWS mask
Barbara	44.6±0.3	51.0±0.4	poor fit
Barbara(1)	37.1±0.5	43.0±0.5	primary
Barbara(2)	21.0±0.2	24.2±0.2	satellite
	a (km)	ρ (mas)	
(1)-(2)	24.2±0.2	28.1±0.2	separation

Table 3: Results from geometric models fits to measured visibilities. Uncertainties are 1σ.

Asteroid	D (km)	p_V	η	θ_D (mas)	Model
Gaspra	13.8±1.0	0.24±0.14	1.06±0.17	22.0±1.6	NEATM
Gaspra	11.6±0.4	0.34±0.13	(0.756)	18.4±0.6	STM
Gaspra	24.0±0.3	0.08±0.04	-	38.1±0.5	FRM
Barbara	51±2	0.17±0.09	1.17±0.05	58±2	NEATM
Barbara	40±1	0.27±0.09	(0.756)	46±1	STM
Barbara	89±1	0.06±0.03	-	102±1	FRM

Table 4: Results from thermal model fits. Uncertainties are at 1σ level. D is the diameter of a sphere with the same projected area visible to the observer; p_V is the geometric albedo in visible light; η is the beaming parameter. An uncertainty of 0.5 magnitudes was assumed on the adopted value of the absolute magnitude H (from the MPC). Values of η in brackets are default values. θ_D is the angular extension of D in mas at the distance of the asteroid.